Title
Insights Into the Causes of Arc Rifting From 2-D Dynamic Models of Subduction

Journal
Geophysical Research Letters, 44(21)

ISSN
0094-8276

Author
Billen, Magali I

Publication Date
2017-11-16

DOI
10.1002/2017gl075061

Peer reviewed

Insights into the Causes of Arc Rifting from 2D Dynamic Models of Subduction

Magali I. Billen

[1]Department of Earth and Planetary Sciences, U. C. Davis, USA

Key Points:

- Spontaneous forearc/arc rifting can occur when there is a broad region of weak material in the overriding plate.
- Positive buoyancy of hot, mantle wedge material drives rifting and can change overriding or subducting plate motion.
- Heating of the subducting crust and overriding plate lithosphere could produce adakites or boninites during rifting.

Corresponding author: M. Billen, `mibillen@ucdavis.edu`

Abstract

Backarc spreading centers initiate as forearc or arc rifting events when extensional forces localize within lithosphere weakened by hydrous fluids or melting. Two models have been proposed for triggering forearc/arc rifting: roll-back of the subducting plate causing trench retreat, or motion of the overriding plate away from the subduction zone. This paper demonstrates that there is a third mechanism caused by an *in situ* instability that occurs when the thin high-viscosity boundary, which separates the weak forearc from the hot buoyant mantle wedge, is removed. Buoyant upwelling mantle causes arc rifting, drives the overriding plate away from the subducting plate, and there is sufficient heating of the subducting plate crust and overriding plate lithosphere to form adakite or boninite volcanism. For spontaneous forearc/arc rifting to occur a broad region of weak material must be present and one of the plates must be free to respond to the upwelling forces.

1 Introduction

The existence of back-arc spreading centers was first recognized from the occurrence of shallow seafloor bathymetry and young crust in the marginal basins of the western Pacific [*Karig*, 1971]. At the same time, it was also proposed that back-arc spreading centers initiate as forearc or arc rifting events, which eventually leaves a remnant volcanic arc (whole or split) on the landward side of the back-arc spreading center [*Karig*, 1970]. Two well-known examples of this arc-rifting process are found in the Tonga-Kermadec and Izu-Bonin-Mariana (IBM) subduction zones (Fig. 1). In the Tonga-Kermadec subduction zone the Lau Basin and Havre Trough are the present-day back-arc spreading centers, whereas the Lau-Colville ridge is the remnant (split) volcanic arc [*Karig*, 1970; *Gill*, 1976; *Clift and ODP Leg 135 Scientific Party*, 1995; *Taylor et al.*, 1996]. In the IBM, there has been two episodes of arc rifting [*Stern et al.*, 2003]. Arc rifting first occurred at approximately 30–25 Ma forming the Palua-Kyushu ridge (remnant arc), followed by back arc spreading in the Shikoku and Parece Vela basins from 30–15 Ma. A second arc rifting event may have started as early at 6–10 Ma [*Stern and Bloomer*, 1992; *Martinez et al.*, 1995] forming the west Mariana ridge (remnant arc) with seafloor spreading on the Mariana Trough starting at 3–4 Ma. In addition, the Izu-Bonin Arc is currently experiencing rifting, which is thought to have started at about 2 Ma [*Taylor et al.*, 1991]. In both these regions volcanism thought to be caused by melting of subducted crust (adakites; *Defant and Drummond* [1990]) or hot, shallow melting of metasomatized peridotites (boninites; *Crawford et al.* [1989]) have been identified and related to the extension or rifting close to the trench [*Crawford et al.*, 1989; *Falloon et al.*, 2008; *Cooper et al.*, 2012; *Meffre et al.*, 2012].

Following the discovery of back-arc spreading centers and forearc/arc rifting, several models were proposed to explain how such an extensional process could occur within the overriding plate near a major convergent boundary. In addition to the overall compressive state of a convergent margin, corner-flow models predict that the overriding plate should be in compression above the arc due to the region of low pressure that forms in the mantle wedge corner [*McKenzie*, 1969; *Sleep*, 1975]. *Karig* [1970] initially proposed that extension would be driven by the buoyant upwelling of hot material from the mantle wedge generated by shear heating. However, as it was later shown that shear heating is not a significant heat source, this buoyancy-driven model was superseded by plate-driven models of extension. Based on early plate motion data, and the ages and orientations of marginal basins in the Pacific, *Jurdy* [1979] proposed that roll-back of the subducting slab caused trench retreat, which then pulled part of the overriding plate seaward and away from the larger overriding plate. In contrast *Molnar and Atwater* [1978] and later *Scholz and Campos* [1995] proposed that a change in motion of the overriding plate away from the convergent margin initiated back-arc spreading. In both models, weakening of the overriding plate is needed to localize extension in the arc (e.g., through melt weakening) or forearc (e.g., through hydrous fluid weakening).

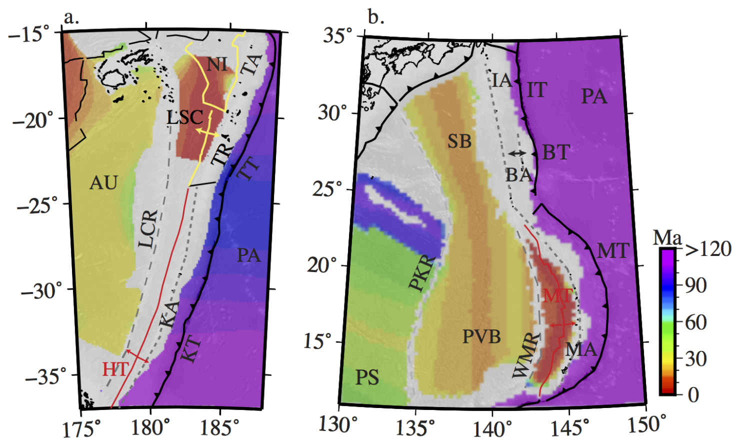

Figure 1. Location of subduction systems with recent arc rifting event(s). Gray-scale is bathymetry [*Smith and Sandwell*, 1997] overlain by transparent color image of seafloor age [*Müller et al.*, 2008]. a) The volcanic arc in Tonga-Kermadec subduction zone began rifting at ≈ 6 Ma to form Lau-Colville ridge (LCR), which is now separated from the active arcs (TA–Tonga Arc, KA–Kermadec Arc) by back-arc oceanic spreading ridges: the Havre Trough (HT) and Lau spreading centers (LSCs). Other labels: TR–Tonga ridge (shallow bathymetric feature), TT–Tonga Trench, KT–Kermadec Trench, PA-Pacific plate, AU–Australian plate, NI–Niafua Plate. b) The volcanic arc of the Izu-Bonin-Mariana subduction systems has rifted twice in the past forming the Palua-Kyushu Ridge (PKR) at ≈ 30–25 Ma and the west Mariana Ridge (WMR) at ≈ 3–4 Ma. The Bonin Arc (BA) is currently rifting. Other labels: IA–Izu Arc, MA–Mariana arc, PVB–Parece Vela Basin, SB–Shikoku Basin, PS–Philippine Sea Plate, PA–Pacific Plate, IT–Izu Trench, BT–Bonin Trench, MT–Mariana Trench.

More recently, analysis of the formation of back-arc basins using plate tectonic reconstructions for the Cenozoic indicates that just prior to the initiation of back-arc spreading, the overriding plate motion changes to move away (retreat) from the subduction zone, supporting the model of overriding-plate driven extension and rifting [*Sdrolias and Müller*, 2006]. However, there is still significant disagreement as to whether deformation in subduction zones is primarily driven by the changes in motion of the overriding plate [*Heuret and Lallemand*, 2005] or the subducting slab [*Schellart*, 2008]. Analysis of such absolute plate motion depends significantly on the choice of reference frame [*Schellart et al.*, 2008], and while the timing of seafloor spreading can be determined from seafloor magnetic anomalies, timing and duration of extension prior to seafloor spreading is more difficult to constrain.

Here, a different mechanism for arc/forearc rifting is presented that is not driven by external changes in plate motions, but instead results from an internal, buoyancy driven extension. This new mechanism occurs under limited conditions in 2D numerical models of subduction in which buoyancy forces drive subduction, plate and trench motions (e.g., fully-dynamic models). Although these models are quite simple in terms of the processes leading to formation of a weak region in the overriding plate, they provide insight into the necessary conditions for spontaneous forearc/arc rifting to occur. The models also facilitate the evaluation of the expected evolution in thermal structure, and therefore also the type of volcanism that might accompany such a rifting event.

2 Modeling Methods

Subduction dynamics is modeled in a two-dimensional (2D) slice of a spherical shell extending from the surface to the core-mantle boundary and 61° in longitude (Fig. S1).

Simulations are run using the CitcomS finite element code [*Zhong et al.*, 2000; *McNamara and Zhong*, 2004; *Tan et al.*, 2006]. The model set-up is identical to *Arredondo and Billen* [2017], allowing for fully dynamic simulations in which only buoyancy forces drive subduction, surface plate and trench motion. That is, there are no imposed velocity or stress boundary conditions: all boundaries are free-slip. In addition a boxed region at the trailing end of both plates with a fixed thermal profile and low viscosity allowing the plates to freely move away from or toward the sidewalls. The minimum element size is 2.5 km by 1.5 km in a 1000 wide by 170 km deep region centered at 35° and increases incrementally into the surrounding domain. Subduction is initiated with a proto-slab extending to a depth of 200 km. In addition, the models include: 1) a layered density structure for the subducting plate, 2) a composite visco-plastic rheology based on laboratory experiments for olivine, and 3) compositionally-dependent phase transitions (which lead to slow folding and bending of the plate, and slow trench advance and retreat). Other details of the model set-up can be found in *Arredondo and Billen* [2017] and Figure S1.

An important aspect of the models for the process of arc rifting is the characterization of the crustal layer on the subducting plate. The overriding and subducting plates are separated by the 7.5 km thick low viscosity basalt crustal layer on the subducting plate. This weak layer acts as the shear zone plate boundary and its location and dip are determined by the evolving dynamics in the simulation. The viscosity of the weak crustal layer is defined such that the specified crustal viscosity (e.g., 10^{20} Pa s) is the maximum viscosity of the shear zone: therefore, if the material gets hotter or the strain-rate increases enough to weaken based on the olivine flow law defined, then that weakening can occur. In addition, the crustal material undergoes a phase transition from basalt to eclogite at depths of 50–150 km (depending on temperature), which also causes the viscosity to transition from that of the weak basalt to a viscosity for strong eclogite (in this case modeled with the same flow law as for olivine).

To summarize the change in stress-state of the overriding plate, the horizontal strain-state (HSS) is calculated. HSS represents the orientation of the principal axis of the strain-rate tensor. Consider the dip of the principal shortening axis at a point in the model domain, $\theta = 0$ to ± 180 (measured counter-clockwise with-respect to the horizontal), then $HSS = \cos(2\theta)$. Therefore, when $\theta = 0$ or ± 180 then $HSS = 1$ representing horizontal shortening. When $\theta = \pm 90$, corresponding to $HSS = -1$, then the shortening axis is vertical and the stretching axis is horizontal. Therefore, an HSS value close to ± 1 indicates horizontal shortening or stretching, while smaller magnitude values indicate a state of stress that is dipping. In addition, its important to note that the high viscosity plate interior usually deforms at very low strain-rates (1×10^{-17} s^{-1}), therefore, when using HSS to evaluate the changing state of strain, the magnitude of deformation is also tracked using the second invariant of the strain-rate tensor, $\dot{\epsilon}_{II}$.

To evaluate the thermal evolution of the subducting slab and mantle wedge thermal profiles are extracted from the model results. For the subducting plate this is done by extracting a smooth contour along the top of the harzburgite layer. For the top of the crustal layer, the location of the harzburgite curve is shifted by 7.5 km in the direction perpendicular to the local orientation of the boundary. The temperature along both contours is then determined using a bilinear interpolation of the temperature from adjacent grid points to the points on the smooth contours. Based on the highest temperature gradients found at the top of the crustal layer (30°C/km) and a horizontal mesh spacing of 2.5 km, the error in the temperature for the top of the crust is estimated to be on the order of 76°: this corresponds to mislocating the boundary by a full mesh element. For the vertical wedge thermal profile at 38.5° longitude no interpolation is required: the temperature is plotted at the mesh grid points.

3 Results

In the process of modeling time-dependent evolution of slab shape, plate and trench motion [*Arredondo and Billen*, 2017] an unusual overriding plate spreading event occurred in one of the models. This model includes an 80 Ma old subducting plate, 40 Ma old overriding plate and a crustal/shear zone viscosity of 10^{20} Pa s (Model 1). The model evolves as expected for about 30 Ma, until the overriding plate suddenly rifts apart (Fig. 2; Movies S1 and S2). Prior to the rifting event, some of the weak crustal material is accreted to the overriding plate slowly forming a broad weak accretionary prism at the surface, and an ≈ 20 km wide weak region extending down almost to the mantle wedge corner. The broader deep zone forms during an episode of trench retreat from 16.5–18.0 Ma, allowing more material into the space between the plates. The weak crustal material is separated from the hot, weak mantle wedge material by a 15–20 km thick zone of cold, higher viscosity ($> 10^{21}$ Pa s) mantle material (Fig. 2a). This material, which is numerically resolved by 5–10 elements (see white box in Fig. 2e), is not advecting with the mantle wedge and acts as a fixed thermal and mechanical boundary layer.

At about 28.6 Ma, the corner of the mantle wedge flow shifts slightly away from the subducting slab, and up into the overriding plate. This slight shift causes the material forming the core of the previously stationary high-viscosity boundary layer to weaken slightly and to be dragged around the mantle wedge corner and down the slab interface (see red contour in Fig. 2e–g; Movie S1). This sudden removal of the high viscosity boundary creates the conditions for spontaneous arc rifting. The hot mantle wedge material is no longer constrained by the high-viscosity boundary, and the positive buoyancy drives the mantle wedge material upward. The upwelling mantle material pushes up into the middle of the broad, low-viscosity accreted material driving the overriding plate away from the subducting plate. The low-viscosity of this region of the overriding plate is a key factor in allowing the buoyancy of the mantle material to push up into the overriding plate.

The main rifting event takes about 4.0 Ma (28.6–32.4 Ma) and leads to 150 km of extension, but slow continued extension and thinning of this region continues and focuses to a clear "back-arc" location at 38.0 Ma until the end of the model at 40 Ma (Fig. 2l). The extended region has a thin weak crustal layer underlain by a thin high viscosity thermal boundary layer. When the extension focuses at 38 Ma, this region thins losing the high-viscosity layer, while the adjacent extended region moves with the overriding plate. Notably, during the rifting process, the subducting plate shifts into trench advance with the slab dip shallowing slightly beneath the extending region. This deformation of the shallow slab is being driven by folding of the slab in the transition zone, and is unaffected by rifting of the overriding plate (Movie S2).

The orientation and magnitude of the strain-rate in the overriding plate further illustrates the spontaneous nature of the plate rifting event. Figure 2 shows the orientation of the principal stretching direction from the strain-rate tensor for individual time steps. Both prior to and during rifting the amount of strain in the high viscosity portion of the plate is low ($< 10^{-16}$ s^{-1}) and the orientation of the strain is neither dominantly horizontal shortening or stretching (HSS < 1 in Fig. 3a). In addition, the direction of motion of the overriding plate changes from slow trench advance to slow trench retreat and back to advance prior to the rifting event (Fig. 3b; Movie S1).

Prior to the rifting event, the stretching axis in the accreted material indicate shearing parallel to the subducting plate, except for a small region of horizontal stretching at the boundary with the overriding plate (longitude of 37.5°) at shallow depth. As the buoyant mantle material begins to rise into the weak crustal material, a broad region of horizontal stretching forms in the accreted material. However, this zone of extension does not reach all the way to the subducting plate: the viscous coupling of material to the sinking slab and dragging of this material by the slab forms a *back-stop* to the upwelling mantle flow.

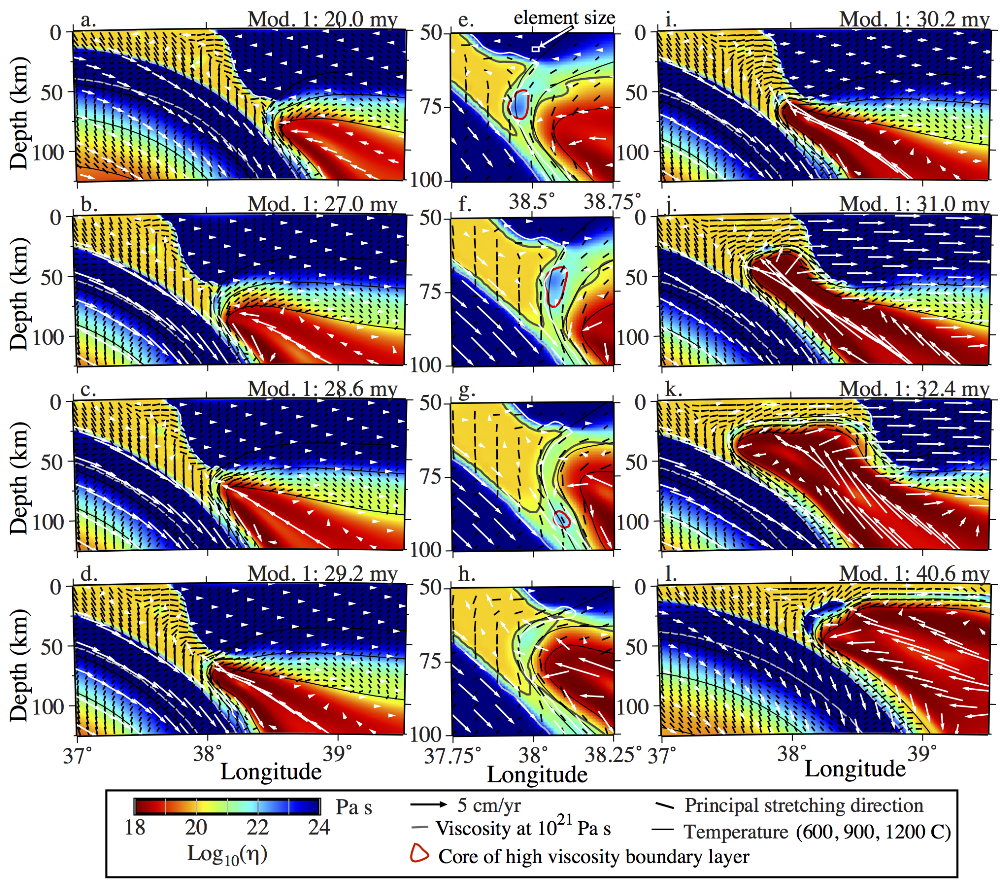

Figure 2. Time evolution of spontaneous arc rifting. a) Subduction corner at 20.0 Ma. b) Just prior (27.0 Ma) to the rifting event the overriding plate is moving slowly towards the subduction zone. c–d and i–k) During the rifting event (29.2–32.4 Ma) rapid upward flow of the mantle pushes the overriding plate, which reverses direction and moves away from the trench and advancing subducting plate. e–h) Zoom-in on mantle wedge corner before (e) and during (f–h) rifting showing advective erosion of thin, high viscosity boundary separating weak forearc from mantle wedge (thick, black contour is viscosity at 10^{21} Pa s; red contour shows core of high viscosity boundary). l) After the rifting event, a high viscosity boundary reforms and subduction continues. Color image shows plate strength (viscosity). Black, thin – temperature contours at 600, 900, and 1200°C. White arrows – flow velocity. Black bars – principal stretching direction from strain-rate tensor. Small white box in (e) shows numerical mesh element size. See also Movie S1.

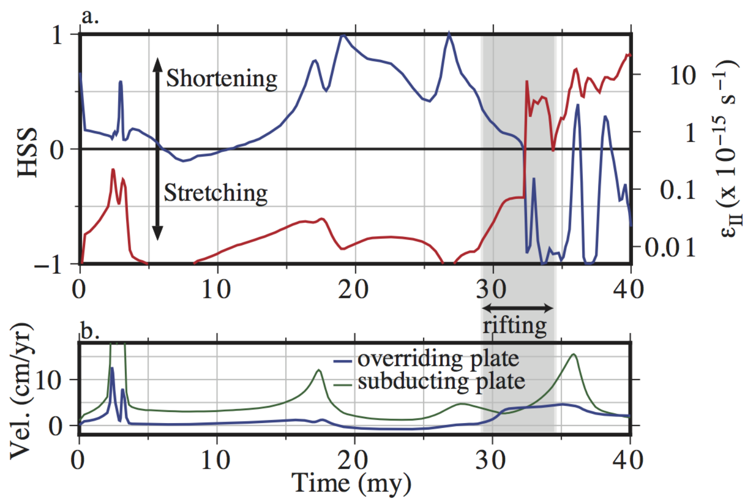

Figure 3. Time evolution of horizontal strain-state (HSS) in the overriding plate represented by tracking a point at 15 km depth and 38.5° longitude. a) Prior to the rifting event at 30.2 Ma, the overriding plate is in a state of very low magnitude horizontal shortening. As rifting occurs, the stress state switches to extension and the magnitude of strain-rate increases 3–4 orders of magnitude. Blue line shows HSS (> 0, shortening; < 0, stretching). Red lines shows magnitude of the strain-rate ($\dot{\epsilon}_{II}$). b) Overriding plate motion (blue) shows slow retreat (negative) from 18–22 Ma, followed by slow advance (positive) from 22–30 Ma, before arc rifting at 30.3 Ma. During rifting the overriding plate moves away from the subducting plate. Subducting plate (green) velocity is responding to bending and buckling of the deeper slab.

Figure 3 shows the evolution of the state of strain in the overriding plate for a representative point at 38.5° longitude and at a depth of 15 km. Using the HSS and second invariant of the strain-rate tensor, it is clear that this region of the overriding plate is in a state of weak compression (shortening) through most of the model evolution prior to the arc rifting event. This state of weak compression is maintained even as the slab and trench undergo episodes of retreat and advance indicating that the overriding plate is primarily moving in response to viscous drag in the mantle rather than coupling along the plate interface. As the rifting event takes place, the strain orientation rotates to horizontal stretching and the strain-rate increases by 3–4 orders of magnitude to $\approx 10^{-14}$–10^{-13} s^{-1} (Fig. 3). After the initial stretching event takes place, there are shifts in the orientation of strain indicating internal deformation of the new thin crustal layer.

During the arc rifting event, the thermal evolution of the slab and wedge records rapid heating of the subducting plate crust and overriding plate lithosphere (Fig. 4). Before the arc rifting event the top of the subducting crust has temperatures of 200–500°C at depths of 50–100 km. At the start of the rifting event the peak temperatures in this same depth range increase to almost 800°C from 29.8–30.7 Ma (Fig. 4b). As the mantle wedge continues to migrate upward, the slab surface remains hot ($T = 800$°C for $z > 50$ km) for another 4.0 Ma before slowly cooling back to pre-rifting temperatures at 36.4 Ma (Fig. 4d). While heating of the slab surface is extreme, there is also a very sharp temperature gradient across the thin crustal layer. During the initial heating, the temperature at the base of the crust (top of the harzburgite layer) only increases by 150° (Fig. 4a). With continued heating, the peak temperature at 100 km eventually reaches 550°C about 5 Ma after the start of the rifting event (Fig. 4c). Finally, extensional thinning of the overriding plate and rapid shallowing of the mantle wedge lead to heating of the overriding plate lithosphere. This heating is initially localized where the mantle wedge first migrates upwards, but eventually, hot temperatures (> 900–1100°) are found at depths of 25–50 km in the region of extended lithosphere.

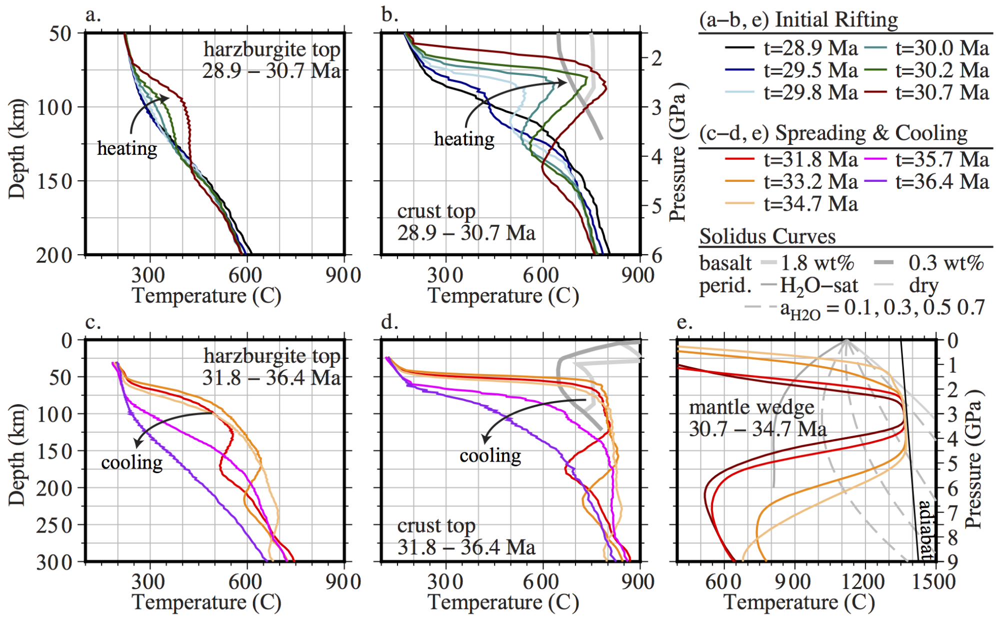

Figure 4. Time evolution of the slab and wedge thermal structure. (a–b) Initial rifting and heating phase (28.9–30.7 Ma). (d–e) Continued rifting and cooling phase (31.8–36.4 Ma). Thermal profiles along the top of the subducting harzburgite layer (base of the crust) (a, c), top of the subducting crust (b, d) and a depth profile through the mantle wedge at 38.5° (e). Solidi for basalt [*Vielzeuf and Schmidt*, 2001] or peridotite [*Hirschmann*, 2000; *Till et al.*, 2010] are shown for comparison to the thermal profiles (see figure legend).

Finally, the spreading event that occurs in this model is dependent on the overall evolution of the model and is therefore sensitive to the properties of both the crustal layer and the overriding plate. For example, there is no spreading event in a model with a higher crustal viscosity (Model 2: 10× larger), which also has slower subduction, a different slab deformation history and different surface plate motions [*Arredondo and Billen*, 2017]. Similarly, no spreading event occurs in a model that is identical to Model 1 except that is has a younger overriding plate (Model 3: 20 Ma). In both cases, there is less accretion of crustal material to the overriding plate (Fig. S2). The subducting plate evolution in both these models (1 and 3) is very similar, with folding events in the slab occurring at the same time with the same time-dependent subducting plate speeds (Fig. S3). Therefore, this type of event is a kind of instability in the system that depends on the particular long-term evolution of the system, and it is not an inevitable consequence of accretion of weak crustal material. In addition, the similar behavior of the slabs in Models 1 and 3, shows that the arc-rifting process occurs independent of the subducting plate behavior at the time of rifting, and also does not interfere with the subduction process. Instead, the only long-term change to the subduction system is the addition of the back-arc spreading center on the overriding plate following the arc-rifting process.

4 Discussion

The model exhibiting spontaneous arc rifting is the only one in which rifting occurred out of a suite of over 40 models that varied subducting plate age (40, 80 Ma), crustal viscosity (10^{20}–10^{21} Pa s), overriding plate age (20, 40 Ma; with or without ridge push), compositional density (with or without), boundary conditions (kinematic, fully-dynamic), and transition zone phase changes [*Arredondo*, 2016; *Arredondo and Billen*, 2016, 2017]. The limited range of conditions in which arc-rifting occurs in the models is due to the potentially unstable nature of the high-viscosity boundary separating the mantle wedge from the weak crustal material. In the models, this high viscosity boundary is fully-resolved, occurring over 5–7 elements. Therefore, while a model with higher resolution might lead to slightly different timing in onset of the arc rifting process, it is not likely to change the overall behavior of the model. Therefore, based on comparison of Model 1 with similar models in which no rifting event occurs, the primary factor leading to spontaneous arc rifting is accumulation (or formation by other means) of a thick region of weak material in the deeper part of the overriding plate just above the mantle wedge corner.

In the model, accumulation of a broad region of weak material requires significant net convergence through either long subduction durations ($>$ 20–40), intermediate to fast subduction rates ($>$ 4 cm/yr), or both. However, the system can remain stable unless the evolution of plate motion and mantle wedge flow leads to thinning of the high viscosity layer that maintains the stable separation of weak forearc material and the hot, buoyant mantle. Such a hot mantle wedge corner, is consistent with modeling of heat flow data across several subduction zones [*Peacock and Wang*, 1999; *van Keken et al.*, 2002; *Currie et al.*, 2004] and the need for hot mantle at shallow depths beneath the volcanic arc [*Kelemen et al.*, 2003]. Therefore, a second important conclusion is that, in stable arcs the strong temperature-dependence of the viscosity may be key to providing the stabilizing barrier in the mantle wedge corner.

Comparison of the evolving thermal structure of the slab and overriding plate to the basalt and peridotite solidus also provides a prediction of the kind of melts that would accompanying this kind of arc rifting event. When compared to the solidus for hydrated basalt, the high slab surface temperatures predict melting of subducting crust at depths ranging between 50–150 km. Such high temperature at shallow depths could produce adakitic volcanism [*Defant and Drummond*, 1990] for almost 5 Ma during the rifting event. At the same time, heating of the interior of the slab would likely result in shallowing of dehydration reactions in the deep crust and shallow harzburgite layer causing rapid release of volatiles [*Hacker*, 2008]. Finally, significant heating of the overriding plate during extension could also cause melting of the lithosphere. Since this material originates above the formerly cold, stable mantle wedge, it is appropriate to consider that it would have been hydrated (e.g., metasomatised peridotite). With this assumption, comparison to the solidi for hydrous peridotite predicts melting at depths of $>$ 25 km and $t > 34.7$ Ma for low water contents ($a_{H_2O} = 0.1$) and more extensive melting that starts earlier ($t = 31.8$ Ma) for higher water contents (i.e., $a_{H_2O} = 0.3$–0.7 to H_2O-saturated; Fig. 4e). Such hot melting of metasomatised peridotite could lead to the formation of boninites [*Crawford et al.*, 1989].

While boninites and adakites have previously been linked to warm slabs (i.e., young, slab edges, slab windows; *Defant and Drummond* [1990]; *Crawford et al.* [1989]; *Yogodinski et al.* [2001]; *Thorkelson and Breitsprecher* [2005]) or slab-break off [*Burkett and Billen*, 2009], the analysis of the model thermal structure presented shows that formation of these melts could instead be driven by instability of the sub-arc mantle and can occur even in systems with cold slabs (e.g., old, $\approx$ 80 Ma), such as Tonga-Kermadec or the IBM. In addition, as in the models, the arc rifting events in these two locations also occurred in well-established subduction systems with oceanic overriding plates, and occurred over short periods of time ($<$ 5 Ma; see Introduction and references therein). Therefore, the subduction system parameters for the arc-rifting model are broadly consistent with the recent occurrence of adakites and boninites in Tonga-Kermadec [*Falloon et al.*, 2008; *Cooper et al.*, 2012; *Meffre et al.*, 2012] and predict that these rock types could have formed in earlier rifting events in both Tonga-Kermadec and the IBM. However, investigation and/or synthesis of the rock types found within the extensional regions formed preceding seafloor spreading in these back-arc basins is needed to further test the applicability of this mode of arc rifting.

One potential weakness of the models used in this study is the simple treatment of the shallow subduction system, which does not explicitly include fluxing of hydrous fluids, melting and melt transport. Therefore, in our models the region of broad weak crustal material acts as a proxy for material weakened by these other processes. In models that include such shallow processes, forearc and arc rifting does occur as a direct result of hydrous and/or melt weakening [*Gerya and Meilick*, 2011; *Vogt et al.*, 2012; *Baitsch-Ghirardello et al.*, 2014], but these models have other limitations because they impose steady motion of the subducting plate and the overriding plate is fixed at the model boundary. Therefore, the models presented here complement these other results because they are fully dynamic and allow for motion of the overriding plate towards/away from the subduction zone.

More importantly, the simple treatment of the overriding plate structure: 1) allows the fundamental requirements for spontaneous arc rifting to be recognized (i.e., a broad weak region above the mantle wedge and a thinning viscous barrier), and 2) demonstrates that the rifting process in these models is not being driven by the slab retreat [*Jurdy*, 1979; *Schellart*, 2008] nor the overriding plate motion [*Molnar and Atwater*, 1978; *Heuret and Lallemand*, 2005; *Sdrolias and Müller*, 2006]. Instead, the dynamical process modeled here represents a new (or forgotten; see *Karig* [1970]) arc rifting mechanism. This new mode of forearc/arc rifting, with its ability to drive plate motion suggests that evaluation of previous and current arc rifting events should not look only to external changes in plate motions prior to rifting, but also to changes in plate motions occurring concurrently with the early stages of arc rifting. For example, there is general agreement between the time-scale of the rifting event and localization to back-arc spreading in the model ($\approx$ 2–5 Ma) and in observations (e.g., as described for the IBM in the introduction). More specifically, while observations from plate tectonic reconstructions indicate that the motion of the overriding plate away from the subduction zone precedes the initiation of arc rifting [*Sdrolias and Müller*, 2006], the time resolution of the reconstructions leaves open the possibility that, in some cases, the change in plate motion occurs as a result of the arc-rifting event itself.

Spontaneous arc rifting is not likely to be the only mechanism for this process in the earth because it requires the overriding plate to be free to respond to the forces from the upwelling mantle wedge (e.g., increased subduction of the overriding plate on a distant subduction zone) or to accommodate this motion on other structures (e.g., reverse faulting on existing weak zones in the overriding plate). For example, the most recent arc rifting event in the Marianas occurred while the trench (and slab) remained relatively fixed. However, motion of the overriding Philippine Sea plate could be accommodated on its western plate boundaries (e.g., the Nankai-Ryukyu trenches in the north and the Philippine and Luzon trenches in the south). In addition, it is possible that spontaneous arc rifting could instead drive trench retreat, if the conditions were suitable at the time of the rifting event. In the models presented, at the time the rifting event occurs the slab and trench motion is being driven by a deeper folding event resulting in trench advance. However, if the overriding plate motion is more restricted [*Baitsch-Ghirardello et al.*, 2014] or the slab/trench motion was at a different phase , then trench retreat may occur instead or in addition to overriding plate motion. Finally, the buoyant upwelling that drives the rifting in these models may also play a role in the evolution of plate-driven forearc/arc rifting. Once the rifting process is initiated, extension will thin the viscous lithosphere allowing buoyant mantle to upwell into weak regions of the lithosphere (e.g., hydrated or having melt).

5 Conclusions

This paper demonstrates that in addition to previous models of forearc/arc rifting driven by motion of the slab/trench or the overriding plate, a third mechanism of spontaneous forearc/arc rifting can occur. This new mechanism is driven by the positive buoyancy of the rising hot mantle wedge material, and requires a broad region of weaker material in the overriding plate above the mantle wedge, and loss of a thin high-viscosity barrier at the mantle wedge corner. Therefore, long-term stability of subduction zones depends on the detailed rheologic structure of the forearc/arc region of the overriding plate. During the rifting process the slab and overriding plate undergo significant heating, which could lead to formation of adakites or boninites, respectively, in a previously cold subduction system. Therefore, identification of these rock types erupted for only a short period of time ($<$ 5 my) within extensional regions formed prior to the onset of back-arc spreading would provide observational support for the model predictions. In addition, the forearc/arc rifting process can modify surface plate motions. Depending on the state of deformation of the slab, forearc/arc rifting could be accommodated by a change to retreating motion of the overriding plate (as in the models presented), by slab/trench retreat or both.

Acknowledgments

The author thanks Christy Till for discussions related to the solidus curves for peridotite and basalt. This manuscript was improved in revision thanks to the critical and thoughtful reviews of the associate editor and an anonymous reviewer. This research was funded by the National Science Foundation award #1246864. The author acknowledges the support of CIG in maintaining the CitcomS software package and GMT 5.0 for figure preparation. The source code and input files used for the models are available in the supplementary information.

References

Arredondo, K., and M. I. Billen (2016), The effects of phase transitions and compositional layering in two-dimensional kinematic models of subduction, *Journal of Geodynamics*, *100*, 159–174, doi:10.1016/j.jog.2016.05.009.

Arredondo, K. M. (2016), The impact of surface bending, a complete mineralogical model and movement of the overriding plate on subduction zones, Ph.D. thesis, University of California Davis.

Arredondo, K. M., and M. I. Billen (2017), Coupled effects of phase transitions and rheology in 2D dynamical models of subduction, *Journal of Geophysical Research*, *122*, doi: 10.1002/2017JB014374.

Baitsch-Ghirardello, B., T. V. Gerya, and J.-P. Burg (2014), Geodynamic regimes of intra-oceanic subduction: Implications for arc extension vs. shortening processes, *Gondwana Research*, *25*, 546–560, doi:10.1016/j.gr.2012.11.003.

Burkett, E. R., and M. I. Billen (2009), Dynamics and implications of slab detachment due to ridge-trench collision, *Journal of Geophysical Research*, *114*(B12402), doi: 10.1029/2009JB006402,.

Clift, P., and ODP Leg 135 Scientific Party (1995), Volcanism and sedimentation in a rifting island-arc terrain: an example from Tonga, SW Pacific, in *Volcanism Associated with extension at Consuming Plate Margins*, edited by J. L. Smellie, pp. 29–51, Geological Society Special Publication No 81.

Cooper, L. B., T. Plank, R. J. Arculus, E. H. Hauri, P. S. Hall, and S. W. Parman (2012), High-Ca boninites from the active Tonga Arc, *Journal of Geophysical Research*, *115*, B10,206, doi:10.1029/2009JB006367.

Crawford, A. J., T. J. Falloon, and D. H. Green (1989), Classification, petrogenesis and tectonic setting of boninites, in *Boninites: and related rocks*, edited by A. J. Crawford, Kluwer Academic Publishers Group.

Currie, C. A., K. Wang, R. D. Hyndman, and J. He (2004), The thermal effects of steady-state slab-driven mantle flow above a subducting plate: the Cascadia subduction zone and backarc, *Earth and Planetary Science Letters*, *223*, 35–48, doi:10.1016/j.epsl.2004.04.020.

Defant, M. J., and M. S. Drummond (1990), Derivation of some modern arc magmas by melting of young subducted lithosphere, *Nature*, *347*, 662–665.

Falloon, T. J., L. V. Danyushevsky, A. J. Crawford, S. Meffre, J. D. Woodhead, and S. H. Bloomer (2008), Boninites and adakites from the northern termination of the Tonga Trench: Implications for adakite petrogenesis, *Journal of Petrology*, *49*(4), 687–715, doi: 10.1093/petrology/egm080.

Gerya, T. V., and F. I. Meilick (2011), Geodynamic regimes of subduction under an active margin: effects of rheological weakening by fluids and melts, *Journal of Metamorphic Geology*, *29*, 7–31, doi:10.1111/j.1525-1314.2010.00904.x.

Gill, J. B. (1976), Composition and age of Lau Basin and Ridge volcanic rocks: Implications for evolution of an interarc basin and remnant arc, *Geological Society of America Bulletin*, *87*(1384-1395).

Hacker, B. R. (2008), H_2O subduction beyond arcs, *Geochemistry, Geophysics, Geosystems*, *9*(Q03001), doi:1029/2007GC001707.

Heuret, A., and S. E. Lallemand (2005), Plate motions, slab dynamics and back-arc deformation, *Physics of Earth and Planetary Interiors*, *149*, 31–51.

Hirschmann, M. (2000), Mantle solidus: experimental constraints and the effects of peridotite composition, *Geochemistry, Geophysics and Geosystems*, *1*(2000GC000070), 1–26.

Jurdy, D. M. (1979), Relative plate motions and the formation of marginal basincs, *Journal of Geophysical Research*, *84*(B12), 6796–6802.

Karig, D. E. (1970), Ridges and basins of the Tonga-Kermadec island arc system, *Journal of Geophysical Research*, *75*(2), 239–254.

Karig, D. E. (1971), Origin and development of the marginal basins in the western Pacific, *Journal of Geophysical Research*, *76*, 2542–2561.

Kelemen, P. B., J. L. Rilling, E. M. Parmentier, L. Mehl, and B. R. Hacker (2003), Thermal structure due to solid-state flow in the mantle wedge beneath arcs, in *Subduction Factory, AGU Monograph*, edited by J. Eiler, American Geophysical Union.

Martinez, F., P. Fryer, N. A. Baker, and T. Yamamzaki (1995), Evolution of backarc rifting: Mariana Trough, 20°–24°N, *Journal of Geophysical Research*, *100*(B3), 3807–3827.

McKenzie, D. P. (1969), Speculations on the consequences and causes of plate motions, *Geophys. J. Royal Astron. Soc.*, *18*, 1–32.

McNamara, A. K., and S. Zhong (2004), Thermochemical structures within a spherical mantle: Superplumes or piles?, *Journal of Geophysical Research*, *109*(B07402), doi: 10.1029/2003JB002847, 2004.

Meffre, S., T. J. Falloon, T. J. Crawford, K. Hoernle, F. Hauff, R. A. Duncan, S. H. Bloomer, and D. J. Wright (2012), Basalts erupted along the Tongan fore arc during subduction initiation: Evidence from geochronology of dredged rocks from the Tonga fore arc and trench, *Geochemistry, Geophysics and Geosystems*, *13*(12), Q12,003, doi: 10.1029/2012GC004335.

Molnar, P., and T. Atwater (1978), Interarc spreading and cordilleran tectonics as alternatives related to the age of subducted oceanic lithosphere, *Earth and Planetary Science Letters*, *41*, 330–340.

Müller, R. D., M. Sdrolias, C. Gaina, and W. R. Rost (2008), Age, spreading rates, and spreading asymmetry of the world's ocean crust, *Geochemistry Geophysics Geosystems*, *9*(4), Q04,006, doi:10.1029/2007GC001743.

Peacock, S. M., and K. Wang (1999), Seismic consequences of warm versus cool subduction metamorphism: examples from Southwest and Northeast Japan, *Science*, *286*, 937–939.

Schellart, W. (2008), Subduction zone trench migration: Slab driven or overriding-plate-driven?, *Physics of Earth and Planetary Interiors*, *170*, 73–88, doi: 10.1016/j.pepi.2008.07.040.

Schellart, W. P., D. R. Stegman, and J. Freeman (2008), Global trench migration velocities and slab migration induced upper mantle volume fluxes: Constraints to find an Earth reference frame based on minimizing viscous dissipation, *Earth-Science Reviews*, *88*, 118–144.

Scholz, C. H., and J. Campos (1995), On the mechanism of seismic coupling and back-arc spreading at subduction zones, *J. of Geophys. Res.*, *100*, 22,103–22,115.

Sdrolias, M., and R. D. Müller (2006), Controls on back-arc basin formation, *Geochemistry, Geophysics and Geosystems*, *7*(4), Q04,016, doi:10.1029/2005GC001090.

Sleep, N. H. (1975), Stress and flow beneath island arcs, *Geophys. J. Int.*, *42*, 827–857.

Smith, W. H. F., and D. T. Sandwell (1997), Global sea floor topography from satellite altimetry and ship depth soundings, *Science*, *277*, 1956–1962.

Stern, R. J., and S. H. Bloomer (1992), Subduction zone infancy: examples from the Eocene Izu-Bonin-Mariana and Jurassic California arcs, *Geological Society of America Bulletin*, *104*, 1621–1636.

Stern, R. J., M. J. Fouch, and S. L. Klemperer (2003), An overview of the Izu-Bonin-Mariana Subduction Factory, in *Inside the Subduction Factory*, edited by J. Eiler, Geophysical Monograph 138, American Geophysical Union.

Tan, E., E. Choi, P. Thoutireddy, M. Gurnis, and M. Aivazis (2006), GeoFramework: Coupling multiple models of mantle convection within a computational framework, *Geochemistry, Geophysics and Geosystems*, *7*(6), Q06,001, doi:10.1029/2005GC001155.

Taylor, B., A. Klaus, G. R. Brown, G. F. Moore, Y. Okamura, and F. Murakami (1991), Structural development of sumisu rift, izu-bonin arc, *Journal of Geophysical Research*, *96*(B10), 16,113–16,129.

Taylor, B., K. Zellmer, F. Martinez, and A. Goodliffe (1996), Sea-floor spreading in the Lau back-arc basin, *Earth and Planet. Sci. Lett.*, *144*, 35–40.

Thorkelson, D. J., and K. Breitsprecher (2005), Partial melting of slab window margins: genesis of adakitic and non-adakitic magmas, *Lithos*, *79*, 25–41, doi: 10.1016/j.lithos.2004.04.049.

Till, C. B., L. T. Elkins-Tanton, and K. M. Fischer (2010), A mechanism for low-extent melts at the lithosphere-asthenosphere boundary, *Geochemistry, Geophysics and Geosystems*, *11*(10), Q10,015, doi:10.1029/2010GC003234.

van Keken, P. E., B. Kiefer, and S. M. Peacock (2002), High-resolution models of subduction zones: Implications for mineral dehydration reactions and the transport of water into the deep mantle, *Geology, Geochemistry and Geophysics*, *3*(10), 1056, doi:10.1029/2001GC000,256.

Vielzeuf, D., and M. W. Schmidt (2001), Melting relations in hydrous systems revisited: application to metapelites, metagraywackes and metabasalts, *Contributions to Mineralogy and Petrology*, *141*, 251–267, doi:10.1007/s004100100237.

Vogt, K., T. V. Gerya, and A. Castro (2012), Crustal growth at active continental margins: Numerical modeling, *Physics of Earth and Planetary Interiors*, *192-193*, 1–20, doi:10.1016/j.pepi.2011.12.003.

Yogodinski, G. M., J. M. Lees, T. G. Churlkova, F. Dorendorf, G. Woerner, and O. N. Volynets (2001), Geochemical evidence for the melting of subducting oceanic lithosphere at plate edges, *Nature*, *409*, 500–504.

Zhong, S., M. T. Zuber, L. Moresi, and M. Gurnis (2000), Role of temperature-dependent viscosity and surface plates in spherical shell models of mantle convection, *J. of Geophys. Res.*, *105*, 11,063–11,082.